Review

Influence of Alloying Materials Al, Cu, and Ca on Microstructures, Mechanical Properties, And Corrosion Resistance of Mg Alloys for Industrial Applications: A Review

Rajadurai Murugesan,* Srikanth Holalu Venkataramana, Siva Marimuthu, Praveena Bindiganavile Anand,* Santhosh Nagaraja,* J. Samson Isaac, R. Raja Sudharsan, T. M. Yunus Khan, Naif Almakayeel, Saiful Islam, and Abdul Razak

Cite This: ACS Omega 2023, 8, 37641−37653

Read Online

ACCESS | Metrics & More | Article Recommendations

ABSTRACT: Magnesium is renowned for its favorable low-density attributes, rendering it a viable choice for commercial engineering applications in which weight has substantial design implications. Magnesium (Mg) stands as a readily obtainable metallic element, exhibiting robustness, efficient heat dissipation, and excellent damping properties. The utilization of pure magnesium remains infrequent due to its susceptibility to instability under high temperatures and pronounced vulnerability to corrosion within humid environments. Hence, the incorporation of magnesium alloys into the design process of aircraft, automotive, and biomedical applications assumes paramount importance. This Review presents a comprehensive review of research endeavors and their resultant achievements concerning the advancement of magnesium alloys. Specifically focusing on aerospace, automotive, and biomedical applications, the Review underscores the pivotal role played by alloying constituents, namely aluminum (Al), copper (Cu), calcium (Ca), and PEO coatings, in influencing the microstructural attributes, mechanical potency, and resistance to corrosion.
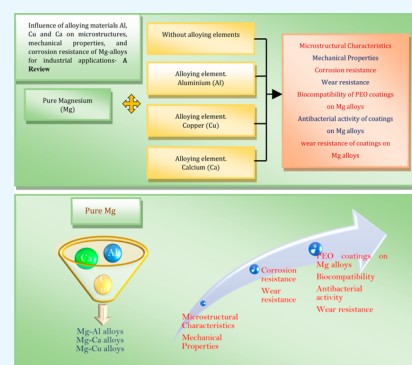
INTRODUCTION

Magnesium, which is abbreviated as the symbol Mg, is a commonly accessible metal with a density of 1.7 g cm^{-3} and an atomic number of 12. It is a more lightweight material than all other structural materials and is usually seen in the oceans of the world. It is seen as a gleaming gray solid. Magnesium and related alloys are difficult to deform at ambient temperature due to the crystal orientation, which is a hexagonal close-packed structure (hcp, Figure 1), and at low temperatures this structure limits the deformation capacity due to it containing slip systems. Magnesium metal has a low melting point, making it simpler to melt for casting. Furthermore, in a marine environment, it is somewhat chemically unstable and highly corrosive. Metal corrosion is thought to be caused by impurities in the metal rather than an inherent property.[1] The purest form of magnesium material is seldom utilized to make aeronautical and automotive products. Therefore, the pure Mg is alloyed with other metals to be employed in various industrial processes. Al, Zn, Ce, Ag, Th, Y, and Zr are some of the most commonly alloyed elements.

The American Society for Testing Materials created a technique for categorizing magnesium alloys to name them. The first two letters in that manner identify the main alloying elements in the composition of the materials, and the next one
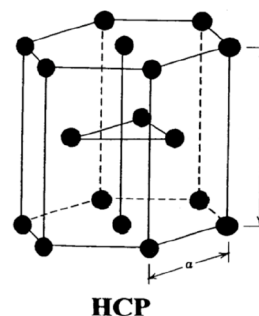

Figure 1. Crystalline structure of hcp magnesium. Adapted from reference 1 with permission. Copyright 2020 Materials Today: Proceedings.

or two letters will be numerals that reflect the amount of alloying elements in wt % of the total weight of the material.

For instance, the alloy code AZ91 represents 9% of Al, 1% of Zn, and the remaining 90% of Mg in the complete alloy composition (Mg−9Al−1Zn).[2]

Magnesium may be alloyed with rare earth elements as well. This will assist the magnesium metal in increasing its strength at high temperatures, and the material is 33% more lightweight than Al, 60% more lightweight than Ti, and 75% more lightweight than steel. Magnesium is utilized to create other metals from their compounds due to being a potent reducing agent (e.g., titanium, zirconium, and hafnium). Magnesium alloys are useful in engineering applications because of their good mechanical properties like high strength, ductility, and creep resistance; their physical properties like low density compared to all other structural materials; recyclability; and low cost to manufacture. Magnesium is a strong and light metal that is ideal for aircraft components.

Mg is also used to make various products, including hand-held devices (like hedge clippers, chain saws, and power tools), products for automobiles (like seat frames, steering wheels and columns, crankcases, transmission cases, gearbox housings, and camshaft sprockets), and electronic equipment (like camcorders, laptop computers, cellular telephones, and TV sets). The benefits of magnesium alloy in casting are as follows: (i) castings with thinner walls than aluminum can be produced (1−1.5 mm vs 2−2.5 mm); (ii) castings cool faster due to the lower latent heat of fusion per unit volume; (iii) due to the low density of magnesium, high gate pressures may be reached at modest pressures; and (iv) iron has limited solubility in the magnesium alloys in casting dies, and any inclination for die soldering is reduced.[1]

PROCESSING OF MAGNESIUM AND ITS ALLOYS

There are several techniques for making magnesium alloys. The methods used most often to make Mg alloys are called the various casting processes, like high-pressure die-casting; in particular, sand mold and permanent mold casting are the most appropriate processes. Squeeze casting, thixocasting, and thixomolding are further important manufacturing methods.[3−5]

At around 2300 °C, the procedure can be accomplished using carbon.

$$2MgO(s) + Si(s) + 2CaO(s) \rightarrow 2Mg(g) + Ca_2SiO_4(s)$$

$$MgO(s) + C(s) \rightarrow Mg(g) + CO(g)$$
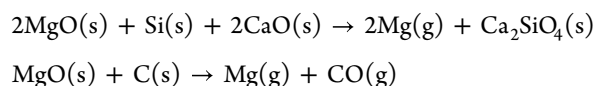
According to the International Magnesium Association (IMA), the use of die-cast magnesium alloys in automobile components is expanding at an unprecedented annual rate. According to this, the market for magnesium alloys will continue to grow the fastest in high-pressure die casting.[6,7]

Although die-casting is the most common method of casting, magnesium alloys are particularly advantageous for sand cast aerospace applications because of their low density and other benefits. For items that must operate at temperatures between 250 and 300 °C for lengthy periods of time, special casting alloys containing Zr are employed. These alloys include zinc, yttrium, silver, and rare earth elements.[8,9]

The cast alloys are predominating over the wrought items, such as forgings, extrusions, plates, and sheets; the latter are also employed in a range of applications. However, recently there has been a resurgence of interest in wrought alloys in the automobile sector as a possible use for magnesium.[7]

In comparison to aluminum alloys, which 50 million tonnes of which are used annually, magnesium alloys were used far less frequently, less than 1 million tonnes annually. This is due to Mg alloy properties like corrosion and creep and burn at high temperatures. As a result of the mixing of numerous metals, magnesium alloys are created. As a result, the created magnesium alloy will have superior properties to magnesium metal.[2]

MAGNESIUM'S REACTION TO VARIOUS ALLOYING ELEMENTS (MG)

The properties of magnesium are modified when other elements are combined with it, and the properties may be improved further by modifying the composition. The assessment in this study is on the various elements when they are alloyed with magnesium.

Pure Magnesium (Mg). The galvanic corrosion of Mg and its alloys is accelerated in their pure forms because of the strong chemical reactivity of Mg or any other alloying elements. In any case, the magnesium matrix acts as the cathode and dissolves in the microgalvanic cells.[7] The purification procedures may significantly reduce the corrosion rate of pure magnesium, as claimed by Song[8] and Ren et al.[9] Limits of impurity tolerance are associated with pure magnesium's corrosion resistance. When the concentration of contaminants goes beyond the tolerance limit, corrosion will happen more quickly. The most dangerous contaminants to the pure magnesium material are iron, copper, and nickel, which have tolerance limits of 170×10^{-6}, 1000×10^{-6}, and 5×10^{-6}, respectively.[10] The technique of manufacturing, as well as the existence of a third ingredient, determines the tolerance limits. Lee et al.[11] proposed the corrosion behavior of the pure magnesium is determined by the impurity of content proportion, such as the Fe/Mn proportion, rather than the impurity content.

Aluminum's Influence (Al). Aluminum is one of the elements frequently alloyed with magnesium, with concentrations ranging from 2 to 9 wt % in commercially available Mg−Al alloys.[12,13] Mg and Al are alloyed to increase strength as well as corrosion resistance.[14,15]

Al is alloyed with Mg[7] to increase the strength of Mg−Al alloys, as well as to strengthen the solid solution and precipitation. Mg−Al alloys have improved castability and higher strength.[16] As the amount of Al increases, the temperatures of the solidus and liquidus lines decrease, which accounts for the improved castability of Mg−Al alloys.[7]

In one study, the elongation percentage of the high-pressure binary die-cast Mg−Al alloy decreased as the addition of aluminum content in increased from 2 to 18 mass %.[7] When these Al concentrations increased, the yield strength values gradually increased, whereas the ultimate strength also increased up to 14% mass %, as shown in the Table 1. Yield strength values improved from 87 to 244 MPa with the increase in aluminum concentration from 2−18%, but the elongation percentage values decreased from 19% to 0.75%, respectively.

The optical microstructures of the Al−Mg specimen consist of the combination of solid solution primary α-Mg and β-$Mg_{17}Al_{12}$ phase particles are presented as shown in Figure 2. The microstructured eutectic β-$Mg_{17}Al_{12}$ phases are developed in the casting sample cooled at high cooling rates with a lower aluminum concentration of 14% Al. The sample prepared with a lower Al concentration, which is less than 9% the eutectic

Table 1. Tensile Characteristic of Binary "Mg−Al" Alloys at Room Temperature (25 °C)[a]

alloy	0.2% YS (MPa)	UTS (MPa)	elongation (%)
Mg−2Al	86.5 ± 1.5	199.5 ± 2.0	18.9 ± 2.6
Mg−5Al	112.1 ± 2.3	236.4 ± 0.9	16.1 ± 3.5
Mg−9Al	147.5 ± 2.9	244.4 ± 7.9	6.2 ± 0.7
Mg−14Al	191.1 ± 3.7	255.5 ± 9.6	1.7 ± 0.3
Mg−18Al	243.8 ± 2.8	253.8 ± 5.4	0.6 ± 0.05

[a]Adapted from reference 7 with permission. Copyright 2008 Elsevier.

phase, was detached, as shown in the Figure 2a and b. The morphology β-Mg^{17}Al^{12} occurs as different particles sizes in this specimen, which is surrounded by the areas of the α-Mg phase, were higher in the Al region than the main α-Mg phase. The eutectic phases vary from completely distributed (Figure 2a) to partially distributed (Figure 2b and c) then to the fibrous mode (Figure 2d and e) with increasing aluminum concentrations from 2% to 18%. The colonies of the α-Mg phase are presented within the β-Mg^{17}Al^{12} phase in a partially separated form, but the two phases of α-Mg and β-Mg^{17}Al^{12} are fully intermixed in the fibrous morphology eutectic structure.

A significant volume proportion of the β-Mg^{17}Al^{12} phases and a refined Mg composition arise from an increase in the number of eutectic phases in the die-cast binary Mg−Al. The eutectic phase fraction is much lower in the 2% Al alloy but in the 18% Al alloys accounts for one-quarter of the eutectic phase fraction in the microstructures. Obviously, the yield strength values are greatly improved; between the Al contents of 2% and 9%, the yield strength was around 180% higher. Due to the finer grain size and rising volume percentages of β-phase particles in the higher volume content of the Al alloys, this strength gain occurs at room temperature.

According to Pettersen et al.,[17] commercially available die-cast high-pressure magnesium alloys like AM60 and AZ91, which include more aluminum than the AM20 alloy, have larger volume fractions of the eutectic phase and hence tend to have a lower elongation percent. There has not been much research done on the effects of aluminum content on the mechanical characteristics and microstructural characteristics of die-cast high-pressure binary Mg−Al alloys. In order to concentrate solely on the role of aluminum in defining mechanical qualities, no other alloying elements were introduced to the melt prior to casting in this study. There was a noticeable decline in ductility as aluminum levels increased (Table 1), which resulted in greater volume percentages of the eutectic phase. As the volume percentage of this brittle phase increases at room temperature, ductility decreases.

The amount of Al in Mg directly affects how quickly Mg−Al alloys corrode, with higher Al percentages frequently resulting in lower corrosion rates.[18−20] The creation of an insoluble Al layer rather than Mg(OH)$_2$, which is easily soluble with the solution chloride, is the reason for better corrosion resistance.[21] Recent research has shown that Mg−Al alloys have better corrosion resistance than pure magnesium with different solutions such as simulated bodily fluids (SBF),[19] phosphate buffer saline (PBS), and sodium chloride (NaCl).[18,20,22,23] Three Mg−Al alloys are compared to pure magnesium in Tafel plots in Figure 3. These findings demonstrate that the three magnesium alloys have superior corrosion resistance compared to pure magnesium. After 16 and 24 days of immersion, the AZ31 alloy outperformed the AZ91 and AZ61 alloys in terms of potential.[19]

Calcium's Influence (Ca). The alloying of magnesium with calcium refines grain sizes,[24−27] resulting in improvement of the mechanical characteristics of Mg at ambient temperature. Calcium has a maximum solubility of 0.8 wt % in the magnesium lattice. The sample with 16.2 wt % calcium content solidifies in the eutectic phase. The optical microstructures of the sample Mg−Ca consists of combinations of the solid solution α-phase (interstitial Ca) and the eutectic phase (α-phase + Mg$_2$Ca$_1$). In an electrochemical reaction, α-Mg is less active than the Mg$_2$Ca$_1$ acting as the anode and the intermetallics acting as the cathode with respect to the element Mg. The crystal structure of Mg$_2$Ca$_1$ is the same as
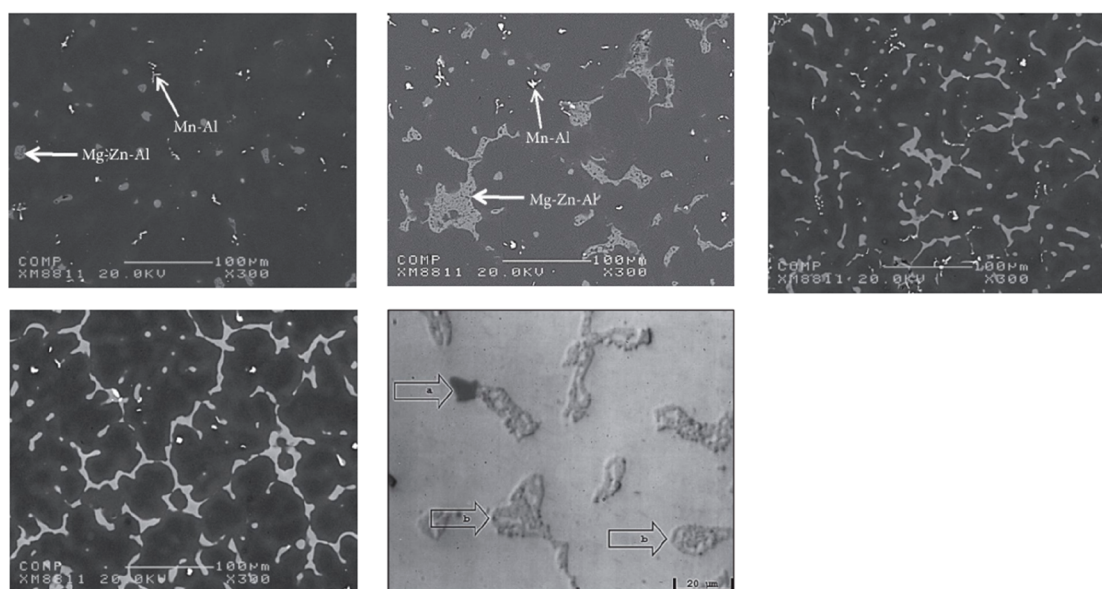

Figure 2. Influence of the aluminum concentration on the microstructure of binary Mg−Al alloys: (a) Mg−4Al, (b) Mg−9Al, (c) Mg−11Al, (d) Mg−14Al, and (e) Mg−18Al. Adapted from reference 16 with permission. Copyright 2017 Advances in Materials Science and Engineering.
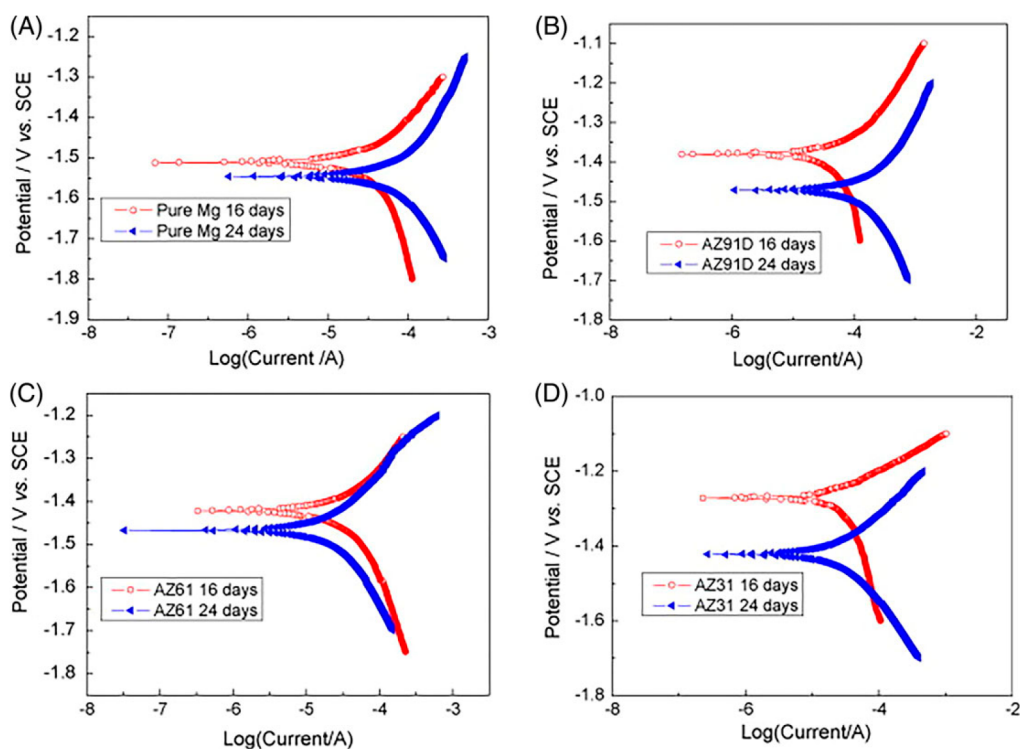
Figure 3. Tafel plots of pure Mg and three Mg−Al alloys after 16 and 24 days of immersion in SBF. (a) Pure Mg, (b) AZ91D, (c) AZ61, and (d) AZ31. Adapted from reference 19 with permission. Copyright 2009 Elsevier.
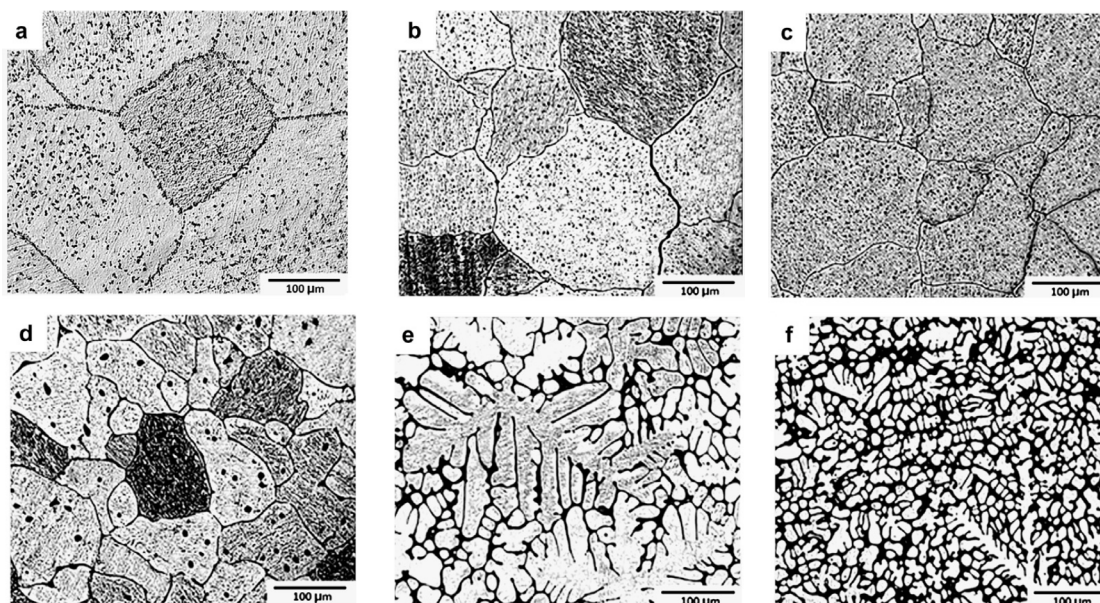

Figure 4. Optical microscopic images of specimens (a) pure Mg and Mg with varying calcium contents: (b) 0.5, (c) 1.25, (d) 2.5, (e) 5, and (f) 10 wt %. Adapted from reference 27 with permission. Copyright 2012 Elsevier.

that of Mg with twice the number of lattice parameters.[28] This reveals that calcium has distinct alloying elements to Mg in the context of biodegradable implants. The addition of a trace quantity of calcium to Mg−Ca alloys has two unique consequences. First, it improves the resistance of corrosion; next, it reduces the development of grains, resulting in smaller grains in castings. The enhanced vulnerability to the development of hot cracks during the process of deformation might be a downside of this grain refinement.[29]

Rad et al.[27] investigated the effect of calcium additions on the microstructures and the characteristics of Mg−Ca alloy with variations of alloying elements Ca in wt % from 0.5 to 10.0 (Figure 4). The microstructural results reveal that with larger concentration of Ca, the intermetallics phases surrounds the grain size especially grain boundaries. These microstructural variations strongly affected the characteristics of the alloys Mg−Ca under quasi static and dynamics conditions by the thermo mechanical heat treatment process.[30] From these microstructural results, the mechanical properties
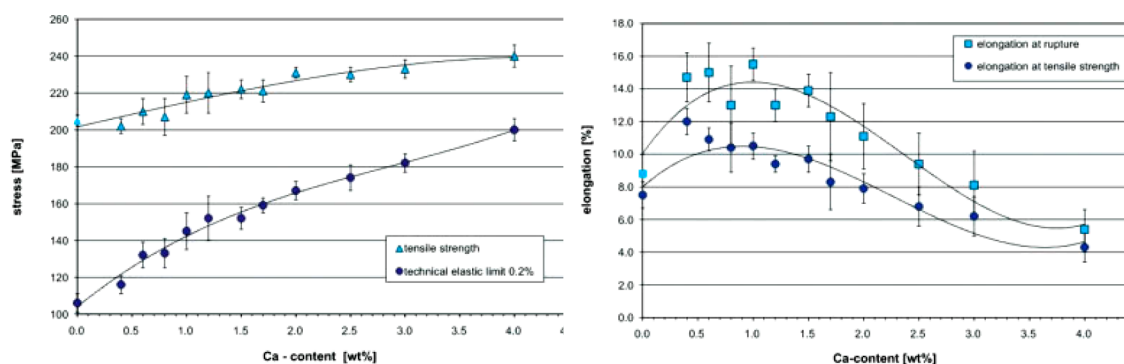
Figure 5. Tensile strength, 0.2% elastic limit, elongation at rupture, and elongation at tensile strength of different Mg−Ca alloys. Adapted from reference 31 with permission. Copyright 2009 Wiley.
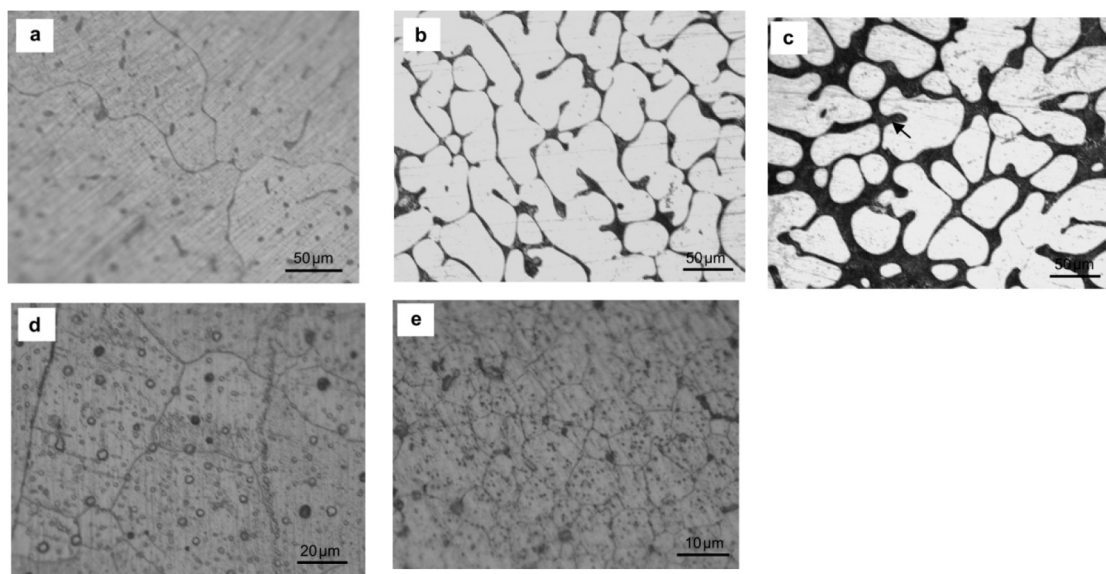

Figure 6. Optical microstructures of (a) as-cast Mg−1Ca alloy, (b) as-cast Mg−2Ca alloy, (c) as-cast Mg−3Ca alloy, (d) as-rolled Mg−1Ca alloy, and (e) as-extruded Mg−1Ca alloy samples. Adapted from reference[32] with permission. Copyright 2008 Elsevier.

elongation percentage of fine grain size structure shows less value as well as the larger grain size structure shows high elongation percentage value. The cell dendritic sizes are decreased with the increase in the Ca additions as well as Mg concentration rise.

Researchers from Drynda et al.[31] and Hassel et al.[29] looked into the impact of calcium concentrations on the mechanical properties and microstructures of binary Mg−Ca alloys. In order to make this particular combination of binary Mg−Ca alloy, the authors blended the pure magnesium (99.8%) and Mg−30Ca pre-alloy (30 wt % Ca) in an appropriate ratio to form binary Mg−Ca alloys with varying Ca concentrations. The mixture of up to 4 wt % alloying element calcium with magnesium shows mechanical properties such as an increased tensile strength of 240 MPa when compared with pure magnesium in the extruded form, which has a tensile strength of about 200 MPa. With the increasing calcium concentration, the 0.2% elastic limit rises progressively. The 0.2% elastic limit for low-alloyed compositions is approximately 80 MPa lower than the value of the tensile strength, which indicates that the plasticity is rather high (Figure 5). Above 2.0 wt % calcium, there is no substantial improvement in tensile strength.

In their 2008 experiment, Li et al. claim binary Mg−Ca alloys were produced for biodegradable materials within bone.

Increasing the Ca concentration causes high-Mg−2Ca phases to develop along the grain boundaries, which weakens the material's mechanical characteristics and the produced Mg−Ca alloy's resistance to corrosion, as shown in Figure 6.[32,27] In Figure 7, the microstructure shows that the refined smaller fine
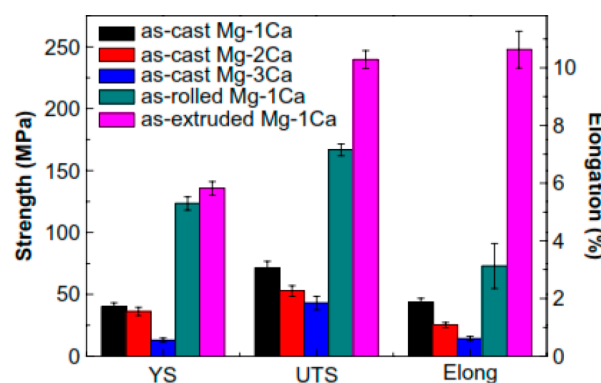

Figure 7. Tensile characteristics of as-cast Mg−1Ca alloy, as-cast Mg−2Ca alloy, as-cast Mg−3Ca alloy, as-rolled Mg−1Ca alloy, and as-extruded Mg−1Ca alloy samples at room temperature. Adapted from reference 32 with permission. Copyright 2008 Elsevier.
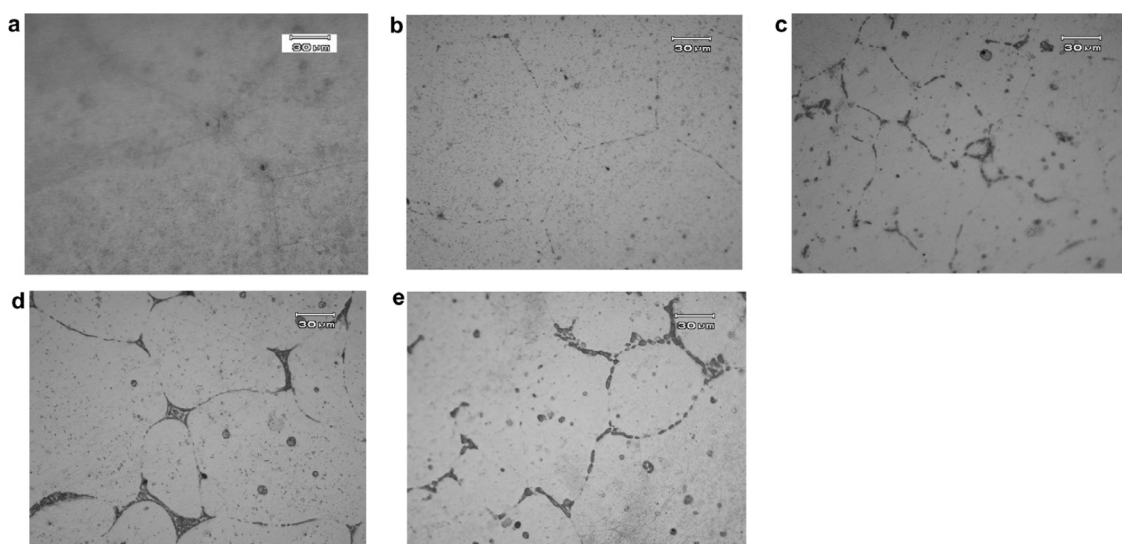
Figure 8. Representative optical micrographs of (a) pure Mg, (b) Mg−0.6Ca, (c) Mg−1.2Ca, (d) Mg−1.6Ca, and (e) Mg−2.0Ca microstructures. Adapted from reference 26 with permission. Copyright 2008 Elsevier.

grain size and structure from the large coarse Mg−2Ca phases after the manufacturing process of hot extrusion or hot rolling. The enhancement of the material's mechanical characteristics and corrosion resistance was greatly aided by these microstructural changes.[32]

The production and characterization of a unique biomedical magnesium−calcium alloy were studied by Wan et al.[26] As shown in Figure 8, microstructural investigations conducted for this work revealed that the quantity and distribution of the Mg−2Ca phase regulate the mechanical properties and corrosion resistance behavior of Mg−Ca alloys.

Excess Mg−2Ca phase reduces the material's mechanical properties like the bending and compressive strengths, as well as the resistance to corrosion. As shown in Tables 2 and 3, the

Table 2. Bending Characteristics of Several Mg−Ca Alloys and Human Cortical Bone[a]

materials	bending strength (MPa)	bending modulus (GPa)	fracture deflection (mm)
pure Mg	95. ± 3	13.9 ± 0.1	18.1 ± 1.7
Mg−0.6Ca	143.3 ± 4.3	15.3 ± 0.4	14.9 ± 0.9
Mg−1.2Ca	132.3 ± 5.3	18 ± 0.2	8.6 ± 1.2
Mg−1.6Ca	130.8 ± 6.5	18.2 ± 0.2	7.8 ± 1.1
Mg−2.0Ca	107.7 ± 5.8	20.9 ± 0.4	5.5 ± 0.9
human cortical bone	179	17.4	

[a]Adapted from reference 26 with permission. Copyright 2008 Elsevier.

Table 3. Compressive Characteristics of Several Mg−Ca Alloys[a]

materials	compressive strength (MPa)	compressive modulus (GPa)	compressive yield point (MPa)
pure Mg	197.9 ± 4.4	44.4 ± 0.7	89.9 ± 6.3
Mg−0.6Ca	273.1 ± 5.9	46.4 ± 0.5	114.3 ± 14.9
Mg−1.2Ca	253.9 ± 7.8	49.5 ± 0.8	96.4 ± 6.5
Mg−1.6Ca	252.4 ± 3.2	54.6 ± 2.3	93.6 ± 7.7
Mg−2.0Ca	232.8 ± 3.6	58.7 ± 1.1	72.9 ± 3.3

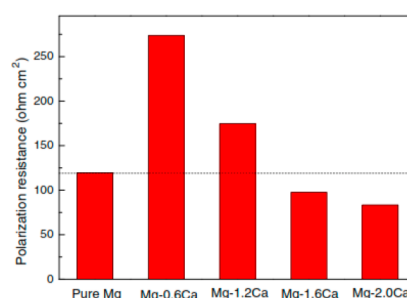[a]Adapted from reference 26 with permission. Copyright 2008 Elsevier.

Figure 9. Polarization resistance of several Mg−Ca alloys. Adapted from reference 26 with permission. Copyright 2008 Elsevier.

optimal Ca content Mg−Ca alloy had greater compressive and bending strengths than the pure Mg. Above the optimal value, the compressive and the bending strengths dropped as the Ca concentration increased. At a low Ca concentration in the alloy, Mg−Ca showed increased tensile strength when compared to the pure Mg.

In addition to enhanced mechanical capabilities, alloying Mg with Ca revealed increased resistance to corrosion compared to pure Mg up to a certain limit.[26,27,31,33] Figure 9 shows that the optimum value of alloying element Ca is up to 0.6 wt % based on the corrosion resistance value, and above the limit of the

inclusion of Ca in Mg decreases the corrosion resistance of the alloys.[26]

Gu et al.[25,34] demonstrated that quickly solidified alloy Mg−3Ca ribbons consist of a fine grain size structure, high resistance to corrosion, and enhanced cell response compared to the casting alloy Mg−3Ca ingots.

Hariprasad Sampatirao et al. and Yun Liu et al. showed the enhancement of the PEO coating efficiency and performance can be achieved through synergistic integration with complementary techniques such as electrophoretic deposition (EPD). This synergy yields the creation of composite films on the Mg substrate,[58−61] exhibiting augmented bioactivity,
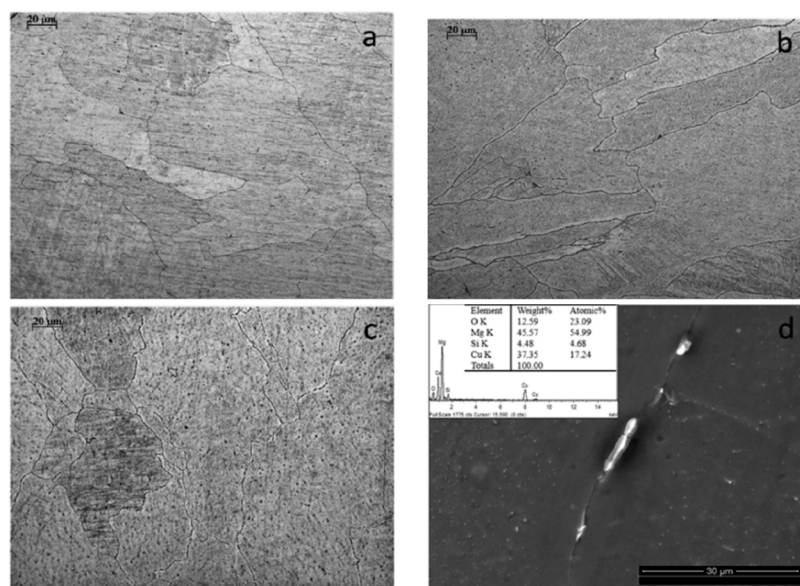
Figure 10. Microstructures of (a) as-cast Mg−0.03Cu, (b) Mg−0.19Cu, and (c) Mg−0.57Cu. (d) Morphology and EDS data from the second phase. Adapted from reference 40 with permission. Copyright 2016 Springer Nature.

heightened corrosion resistance, antimicrobial attributes, and other favorable properties. Notably, the amalgamation of PEO-EPD processes within electrolyte systems containing ZrO_2, TiO_2, CeO_2, and hydroxyapatite particles has proven adept at producing nanocomposite layers with superior characteristics. EPD on a porous substrate is advised for best results in order to make use of the generated MgO layer from PEO62. Charged particles, such as Ag, Zr, Ti, F, Si, Cu, and Ce, are dissolved in the electrolyte during EPD, migrating toward the anode under the influence of sufficiently high potentials. These particles then become integrated into the PEO coating,[62] with their velocity contingent upon the applied voltage and particle radius.[63] The technique is conventionally employed for the deposition of bioactive ceramics onto metallic biomaterials.[64] A notable instance is the work of Razavi et al.,[65] wherein the combined PEO-EPD procedure led to the development of a nanostructured fluoride hydroxyapatite coating (FHA) on AZ91 Mg alloy. The resultant coating exhibited heightened corrosion resistance and bioactivity compared to both bare and exclusively PEO-coated Mg alloys.[66]

Copper's Influence (Cu). Cu is a less expensive element than several rare earth elements like Nd, Ce, Gd, and Y.[35] Cu, on the other hand, helps to improve the characteristics of Mg alloys. It is commonly accepted that the inclusion of Cu enhances castability and effectively boosts the alloy's eutectic temperature, enabling the complete dissolution of solute atoms at high temperatures.[36,37] Additionally, the dissolved atoms of the element Cu appear to enhance nucleation, limit grain expansion, and increase precipitate concentration during aging treatment. Because of the refinement of grains generated by Zn and Cu, the alloy Mg−Zn−Cu has been observed to have good ductility and strength.[38] Zhu et al.[39] looked at how copper additions to alloys affected the microstructural features and mechanical qualities of cast ZK60 magnesium alloy products. The results reveal that the addition of the alloying element copper (0.5−1 wt %) to magnesium produces strong mechanical properties, particularly an exceptional elongation percentage of more than 9%. As a result, at room temperature the mechanical properties of the materials magnesium alloys

are highly enhanced due to the variation of the microstructure, which means that the refinement of grains in the microstructures is strongly influenced by the inclusion of copper with magnesium.

Liu et al.[40] studied the impact of adding copper as an alloying element with main element magnesium on the microstructural characteristics and mechanical performance of three alloys developed with mixing proportions of copper such as 0.03, 0.19, and 0.57. The Figure 10a−c shows that the microstructures of the magnesium alloys consist of the mixed proportion of the fully developed primary matrix, and the secondary granular phases were present.

As illustrated in the microstructures in Figure 10a and b, the minor quantities of the secondary phases are precipitates in the grains, which are visible as black dots. When the amount of copper added as the alloying element in the main element magnesium increased, the amount of secondary phase particles also increased, which is apparent in the grains, and there is no evidence of even distribution or distribution on the grain boundaries (Figure 10c). As per the results EDS (Figure 10d) and the binary phase alloy Mg−Cu diagram, the intermetallic Mg−2Cu phase is the sole precipitates in the whole alloy.

Figure 11 depicts the ultimate tensile strength (UTS), ultimate compressive strength (UCS), and Vickers hardness (HV) of the fully developed Mg−xCu alloys, where x is 0.03, 0.19, and 0.57 wt % copper. The results reveals that the out of the three magnesium copper alloys, the 0.57% copper addition in magnesium shows a high Vickers hardness, with a value of of 38.12 HV, compared to the pure magnesium material, which is about 31.53 HV, and the magnesium alloys with 0.03 (31.94 HV) and 0.19 (37.10 HV) wt % copper composition. The ultimate tensile strength of the 0.57 wt % copper composition alloy (104 MPa) is higher than that of pure magnesium (63.33 MPa), which is more than 200%. This is the cause of the increase in the Mg−2Cu phase around the grain boundaries as well as the resulting pinning process. The UCS of the 0.03 wt % composition (199.67 MPa), in contrast to the UTS and HV, exhibits the greatest value when compared to all other alloys and pure magnesium (185.67 MPa) material. In conclusion,
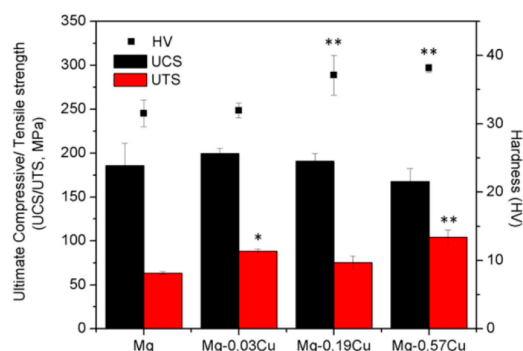
Figure 11. HV, UCS, and UTS of as-cast Mg−Cu alloys. Compared to pure Mg, *p = 0.05 and **p = 0.01. Adapted from reference 40 with permission. Copyright 2016 Springer Nature.

Mg−Cu alloys perform better mechanically than Mg materials without the addition of Cu.

Figures 12 and 13 illustrate the resistance of the alloys Mg−xCu alloys to corrosion as listed above. Figure 12a depicts the pH fluctuation of magnesium−copper alloys and the pure Mg during immersion in the Hank's solution. In the early stage, there is a slow increasing tendency that reaches a climax after one day owing to hydroxyl. As corrosion progresses, additional degraded materials cover over the entire samples, slowing the rate of corrosion and stabilizing the pH values. Figure 12a shows that the pH values of the magnesium copper alloys throughout the immersion period are invariably greater than those of the pure magnesium element. For instance, Mg−0.57Cu has highest rate of corrosion, demonstrating that the additional amount of copper leads to greater corrosion.

Figure 12b displays corrosion rates and pictures of pure magnesium and magnesium−copper alloys after three and seven days of immersion. The Mg−Cu alloys start to corrode substantially more quickly than pure Mg after three and seven days, with Mg−0.57Cu showing the worst corrosion. In contrast to the completely uninjured pure Mg surface, a substantial number of corrosion pits had developed after three days of immersion. Both the Mg−Cu alloys and pure Mg exhibit pitting corrosion after seven days, with the Mg−Cu alloys exhibiting more severe erosion, proving that Cu alloying speeds up Mg corrosion.

The quantity of Mg and Cu liberated from Mg−Cu alloys at various immersion durations in Hank's solution is shown in Figure 13. As shown in Figure 13a, the amount of magnesium

released from Mg−Cu alloys and pure magnesium grows approximately linearly with time, with Mg−0.57Cu having the largest amount. The rate of release from pure magnesium is comparable to that of the alloy Mg−0.03Cu during the first 24 h but significantly slower than those of Mg−0.19Cu and Mg−0.57Cu.

The release rates of Mg−0.03Cu and Mg−0.19Cu alloys are lower than those of pure Mg due to the formation of a shield made up of corrosion products. The pH fluctuation in Figure 12a and these findings are consistent. Figure 13b illustrates how Mg−0.57Cu has the largest Cu release, followed by Mg−0.19Cu and Mg−0.03Cu. The Cu concentration changes slowly in the beginning but dramatically increases after 24 hours.

Zhu et al. looked into how Cu addition affected the microstructure and mechanical properties of the magnesium alloy ZK60 (Mg−6Zn−0.5Zr). The microstructure of the Cu-free alloy (Figure 14a) consists of secondary phases, Mg, and a few solitary particles inside the primary dendrites. At grain boundaries, secondary phases with continuous or semi-continuous morphology can be detected.

As seen in Figure 14b, despite the microstructure being slightly more polished, adding 0.5% Cu to the ZK60 alloy significantly increases the amount of continuous eutectic phases, and the microstructure has a considerable number of isolated particles inside the grains, continuous eutectic phases, and Mg. Enormous dendritic granules and the tiny dendritic grains are the two primary morphologies of the Mg granules. The form of the eutectic phases completely changes to a continuous network when the Cu content is steadily increased to 1.0%.

Similar to this, there are still basic grains with various morphologies. In addition, the grain size is considerably lower than it was for the alloy containing 2% Cu. As the Cu content is increased to 2%, it is evident from Figure 14(d) that the alloy's grain size is the lowest among those of the supplied alloys (see Figure 14a−c). Near grain boundaries, large eutectic phases commonly accumulate.

This is mostly due to the fact that more Cu can be added without significantly altering the kinetics of the precipitation reaction, increasing the driving force of nucleation and resulting in more precipitates.[41] The grain sizes of cast alloys are significantly influenced by the Cu content. The tendency of ZK60 alloys to refine their grain size increases as the amount of Cu added increases (Figure 14). These elements help to
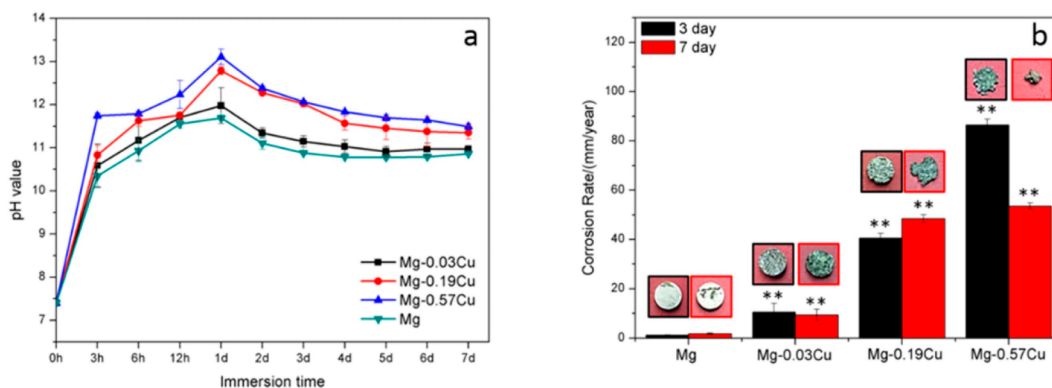

Figure 12. (a) pH change in Hank's solutions and (b) corrosion rates after three days and seven days. Adapted from reference 40 with permission. Copyright 2016 Springer Nature.
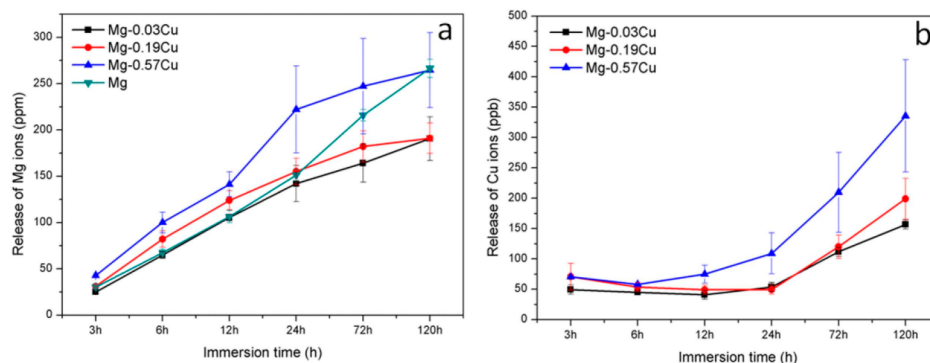
Figure 13. (a) Mg release and (b) Cu release over different immersion periods in Hank's solution. Adapted from reference 40 with permission. Copyright 2016 Springer Nature.
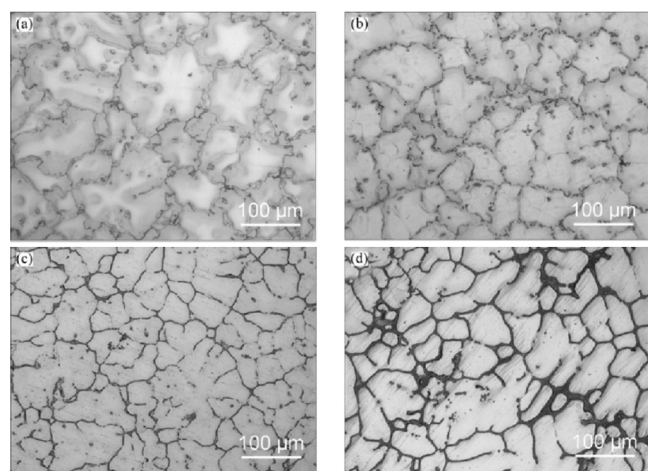

Figure 14. Optical microstructures of as-cast ZK60−xCu alloys: (a) x = 0, (b) x = 0.5, (c) x = 1, and (d) x = 2. Adapted from reference 39 with permission. Copyright 2014 Elsevier.

Figure 15. Room-temperature tensile properties of as-cast ZK60−xCu alloys. Adapted from reference 39 with permission. Copyright 2014 Elsevier.

explain this. On the one hand, the presence of Cu can alter the solidus of the alloys, accelerating their rate of solidification and enhancing their microstructure.[42]

The quantity and distribution of intermetallics are closely correlated with mechanical properties.[43] The intermetallic morphology of ZK60 alloys with trace quantities of Cu changes, affecting the mechanical properties. Figure 15 shows the variations in the tensile properties and elongation to fracture of ZK60 alloys with various Cu concentrations under room temperature tensile conditions (E_f).

The inclusion of Cu has a favorable impact on the tensile characteristics of the tested alloys, as shown by Figure 15. The tensile characteristics are noticeably superior to the alloy with less Cu. It has been discovered that the UTS and E_f initially rise and then reduce when the Cu content increases. When 0.5% Cu is added to ZK60 alloy, the YS and UTS immediately increase compared to the base, but the E_f does not climb to the same level. When the Cu concentration is raised to 1%, E_f reaches its maximum value compared to the 0.5% Cu alloy. The UTS and E_f are increased by 185 MPa and 11.3%, respectively, in comparison to the Cu-free alloy.

Refined grains are widely accepted to enhance the tensile properties[43] of technical alloys.[44] Additionally, as far as we are aware, a number of binary Mg−Zn alloys have had issues with microstructural inhomogeneity.[45] The improvement in tensile properties is due to the Cu addition's ability to efficiently
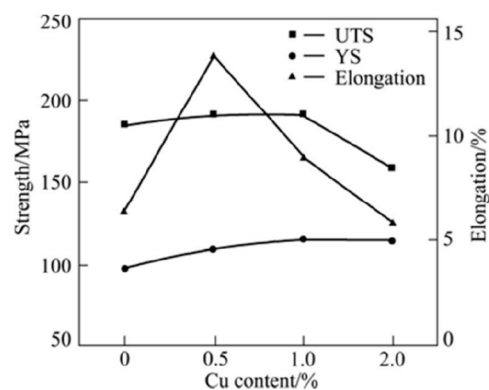
reduce the alloys' grain sizes and address the microstructural inhomogeneity of the alloys under study.

When the Cu level exceeds 1%, the UTS and E_f often decrease. When Cu addition approaches 2%, the UTS and E_f drop from high values of 190 MPa (1% Cu) and 11.5% (1% Cu) to 160 MPa and 6.5%, respectively. A greater Cu inclusion of 2% resulted in the formation of Mg−2Cu compounds and an increase in eutectic phase amounts, which are the main causes of tensile property degradation. Furthermore, during tensile testing, the eutectic morphology transforms into a lamellar or dendritic structure, which acts as a site for fracture initiation and reduces the tensile capabilities.

This is mostly caused by the development of a sizable stress concentration near a sizable number of second phases,[46−51] which may cause fractures to form and mechanical characteristics to deteriorate. Additionally, as the Cu concentration increases, agglomerates continuously surround the main Mg grains, which is predicted to diminish the tensile properties.[52−57]

In essence, the loss of tensile properties is caused by continuous agglomeration and the dendritic shape of the lamellar structure. A sufficient Cu content (0.5 and 1%) can greatly increase the tensile capabilities of as-cast ZK60 base alloys at room temperature, according to an analysis of the characteristics of the tested alloys.

As shown in Figure 16a, the alloy deficient in Cu exhibits a number of porosities as well as numerous tear ridges and cleavage planes. Because there is a dearth of molten metal in some areas, porosities are formed there. The subsequent
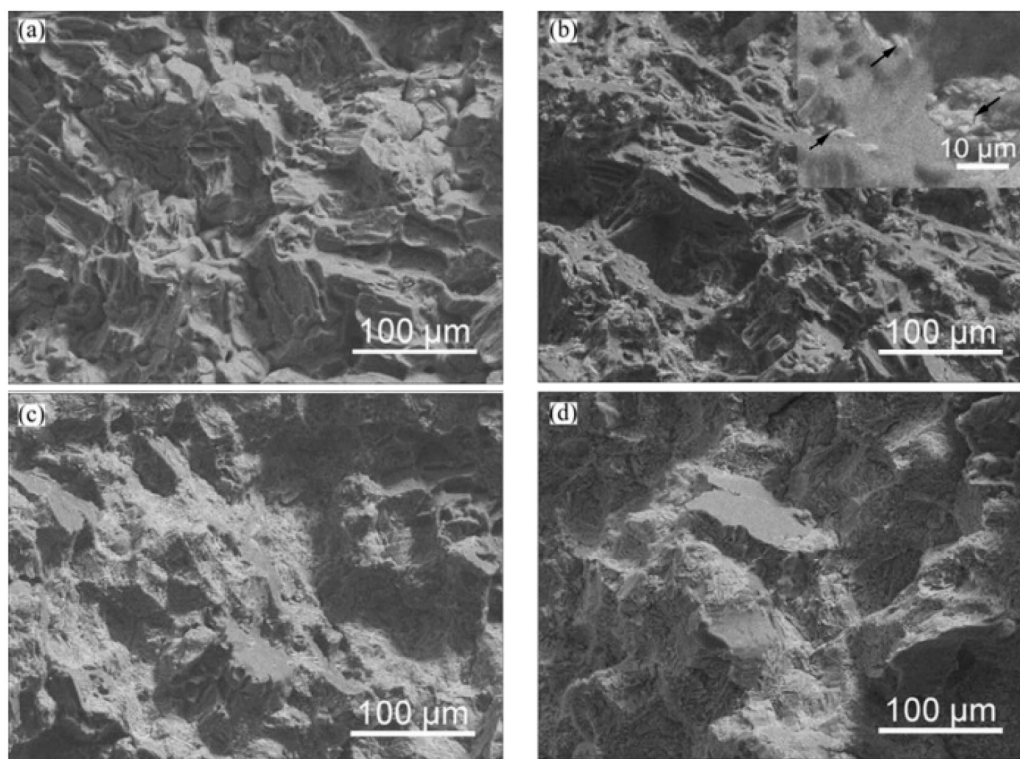
Figure 16. Tensile fracture surface SEM micrographs of as-cast ZK60−xCu alloys: (a) x = 0, (b) x = 0.5, (c) x = 1, and (d) x = 2. Adapted from reference 39 with permission. Copyright 2014 Elsevier.

solidification procedure does not fill these porosities with the proper molten metal due to the comparatively rapid cooling rate. According to their fracture behavior, the Mg−6Zn−-(0−2.5)Cu alloys exhibit cleavage fracture, but the alloy containing 0.5% Cu displays a mixed fracture of intergranular and quasi-cleavage fracture in addition to ductile rupture.

Fattah-alhosseini, et al. studied the process of plasma electrolytic oxidation (PEO), which holds significant promise in enhancing the antibacterial efficacy of magnesium (Mg) implants by utilizing an electrolyte infused with antibacterial agents.[67,68] Introduction of additives based on silver (Ag) or copper (Cu) into the electrolyte induces the integration of these components into the resultant coatings, leading to the controlled release of Ag⁺ ions[69] and Cu²⁺ ions[70] during the incubation process. This confers a bacteriostatic effect upon PEO coating. Released Ag⁺ ions interact with the bacterial cell membrane, instigating bactericidal action. Notably, Ag⁺ ions disrupt the bacterial envelope and engage with organic moieties and enzymatic thiols, thereby perturbing normal bacterial permeability and respiration, and even engage with sulfur- or phosphorus-containing compounds in the DNA of bacteria.[71] Conversely, Cu exerts bactericidal effects through a cascade of interactions. Initially, electrostatic forces facilitate the absorption of Cu ions onto the bacterial cell membrane and impede bacterial activity, which triggers metabolic anomalies and eventual cellular demise. Subsequently, Cu ions infiltrate the bacterial membrane, inducing membrane destabilization; this results in cytoplasmic leakage and cellular demise. Furthermore, Cu ions interfere with respiratory chains and disrupt the bacterial gene replication process. Ultimately, the cytotoxicity of Cu²⁺ ions arises from their displacement of iron atoms from iron−sulfur clusters, leading to impairment of essential catabolic and biosynthetic pathways.[72] Noteworthy is

the potential for cytotoxicity resulting from excessive Cu and Ag ion concentrations.[73−75]

The postproduction surface alteration of magnesium (Mg) and its alloy counterparts, subsequent to generating robust, porous, and substantial coatings through the plasma electrolytic oxidation (PEO) method, has resulted in significant enhancements in the wear resistance of the materials. The infusion of additives into solutions, followed by their integration into the coatings, has notably contributed to a further elevation in the wear-resistant properties of PEO coatings applied onto magnesium substrates.[76]

CONCLUSIONS

The influence of Al, Ca, and Cu on the microstructures, characteristics, and corrosion resistance of magnesium alloys are critically reviewed in this article. All of the alloying elements show the best mechanical properties and corrosion resistance ratings when their compositional levels are up to 2% with pure Mg. The microstructure of Mg alloys is significantly influenced by the alloying elements, which tends to improve characteristics as compared to pure Mg.

AUTHOR INFORMATION

Corresponding Authors

Praveena Bindiganavile Anand − *Department of Mechanical Engineering, Nitte Meenakshi Institute of Technology, Bangalore, Karnataka 560064, India*; Email: praveena404@gmail.com

Rajadurai Murugesan − *Department of Aeronautical Engineering, Nitte Meenakshi Institute of Technology, Bangalore, Karnataka 560064, India*; Email: mrajadurai700@gmail.com

Santhosh Nagaraja − *Department of Mechanical Engineering, MVJ College of Engineering, Bangalore, Karnataka 560067, India*; Email: santhoshmvj89@gmail.com

Authors

Srikanth Holalu Venkataramana − *Department of Aeronautical Engineering, Nitte Meenakshi Institute of Technology, Bangalore, Karnataka 560064, India*

Siva Marimuthu − *School of Digital, Technologies and Arts, Staffordshire University, Stoke on Trent ST42DF, United Kingdom*

J. Samson Isaac − *Department of Biomedical Engineering, Karunya Institute of Technology and Sciences, Coimbatore, Tamil Nadu 641114, India*

R. Raja Sudharsan − *Department of Biomedical Engineering, Sri Shanmugha College of Engineering and Technology, Morur, Tamil Nadu 637304, India*

T. M. Yunus Khan − *Department of Mechanical Engineering, College of Engineering, King Khalid University, Abha 61421, Saudi Arabia;* orcid.org/0000-0002-9242-7591

Naif Almakayeel − *Department of Industrial Engineering, King Khalid University, Abha 61421, Saudi Arabia*

Saiful Islam − *Civil Engineering Department, College of Engineering, King Khalid University, Abha 61421, Saudi Arabia*

Abdul Razak − *Department of Mechanical Engineering, P. A. College of Engineering, Mangaluru, Karnataka 574153, India;* orcid.org/0000-0001-7985-2502

Complete contact information is available at:
https://pubs.acs.org/10.1021/acsomega.3c03417

Notes

The authors declare no competing financial interest.

REFERENCES

(1) Jayasathyakawin, S.; Ravichandran, M.; Baskar, N.; Anand Chairman, C.; Balasundaram, R. Mechanical properties and applications of Magnesium alloy − Review. *Materials Today: Proceedings.* **2020**, *27* (2), 909−913.

(2) Polmear, I. *Light Alloys: From Traditional Alloys to Nanocrystals*, 4th ed.; Elsevier: Amsterdam, The NEtherlands, 2005; pp 103−109.

(3) Aghion, E.; Bronfin, B. Magnesium alloys development towards the 21st century. *Material Science Forum* **2000**, *350−351*, 19−30.

(4) Polmear, I. J. *Light Alloys: Metallurgy of the Light Metals*, 3rd ed.; Halsted Press: New York, NY, 1996; pp 362−368.

(5) Magers, D.; Willekens, J. Global Outlook on the Use of Magnesium Diecastings in Automotive Applications. In *Magnesium Alloys and their Applications*; Mordike, B. L., Kainer, K. U.; Werkstoff-Informationsgesellschaft: Frankfurt, Germany, 1998; pp 105−109.

(6) Westengen, H. Magnesium alloys for structural applications; recent advances. *J. Phys. IV France* **1993**, *3*, C7-491−C7-501.

(7) Witte, F.; Hort, N.; Vogt, C.; Cohen, S.; Kainer, K. U.; Willumeit, R.; Feyerabend, F. Degradable biomaterials based on magnesium corrosion. *Curr. Opin. Solid State Mater. Sci.* **2008**, *12*, 63−72.

(8) Song, G. L. Control of biodegradation of biocompatible magnesium alloys. *Corros. Sci.* **2007**, *49*, 1696−1701.

(9) Ren, Y. B.; Huang, J. J.; Yang, K.; Zhang, B. C.; Yao, Z. M.; Wang, H. Study of biocorrosion of pure magnesium. *Acta Metall. Sin.* **2005**, *41*, 1228−1232.

(10) Makar, G. L.; Kruger, J. Corrosion of magnesium. *Int. Mater. Rev.* **1993**, *38*, 138−153.

(11) Lee, J. Y.; Han, G.; Kim, Y. C.; Byun, J. Y.; Jang, J. I.; Seok, H. K.; Yang, S. J. Effects of impurities on the biodegradation behaviour of pure magnesium. *Metals and Materials International* **2009**, *15*, 955−961.

(12) Riaz, U.; Shabib, I.; Haider, W. The current trends of Mg alloys in biomedical application-A review. *Journal of Biomedical Materials Research Part B: Applied Biomaterials* **2019**, *107*, 1970−1996.

(13) Wenwen, D.; Yangshan, S.; Xuegang, M.; Feng, X.; Min, Z.; Dengyun, W. Microstructure and mechanical properties of Mg−Al-based alloy with calcium and rare earth additions. *Mater. Sci. Eng., A* **2003**, *356*, 1−7.

(14) Brar, H. S.; Platt, M. O.; Sarntinoranont, M.; Martin, P. I.; Manuel, M. V. Magnesium as biodegradable and bioabsorbable material for medical implants. *JOM* **2009**, *61*, 31−34.

(15) Bamberger, M.; Dehm, G. Trends in the development of new Mg alloys. *Annu. Rev. Mat Res.* **2008**, *38*, 505−533.

(16) Abdelaziz, M. H.; Paradis, M.; Samuel, A. M.; Doty, H. W.; Samuel, F. H. Effect of Aluminum Addition on the Microstructure, Tensile Properties, and Fractography of Cast Mg-Based Alloys. *Adv. Mater. Sci. Eng.* **2017**, 7408641.

(17) Pettersen, K.; Bakke, P.; Albright, D. Magnesium Die Casting Alloy Design. In *Magnesium Technology*; Kaplan, H. I., Ed.; TMS-AIME: Warrendale, PA, 2002; pp 241−246.

(18) Esmaily, M.; Blücher, D. B.; Svensson, J. E.; Halvarsson, M.; Johansson, L. G. New insights into the corrosion of magnesium alloys-The role of aluminium. *Scripta Mater.* **2016**, *115*, 91−95.

(19) Wen, Z.; Wu, C.; Dai, C.; Yang, F. Corrosion behaviours of Mg and its alloys with different Al contents in a modified simulated body fluid. *J. Alloys Compd.* **2009**, *488*, 392−399.

(20) Pardo, A.; Merino, M. C.; Coy, A. E.; Arrabal, R.; Viejo, F.; Matykina, E. Corrosion behaviour of magnesium/aluminium alloys in 3.5wt.% NaCl. *Corros. Sci.* **2008**, *50*, 823−834.

(21) Walker, J.; Shadanbaz, S.; Woodfield, T. B. F.; Staiger, M. P.; Dias, G. J. Magnesium biomaterials for orthopaedic application: A review from a biological perspective. *J. Biomed Mater. Res. Part B Appl. Biomater* **2014**, *102*, 1316−1331.

(22) Singh, I. B.; Singh, M.; Das, S. A comparative corrosion behaviour of Mg, AZ31 and AZ91 alloys in 3.5% NaCl solution. *J. Magnes Alloy* **2015**, *3*, 142−148.

(23) Wang, L.; Shinohara, T.; Zhang, B. P. Corrosion behaviour of Mg, AZ31, and AZ91 alloys in dilute NaCl solutions. *J. Solid State Electrochem* **2010**, *14*, 1897−1907.

(24) Li, N.; Zheng, Y. Novel Magnesium Alloys Developed for Biomedical Application: A Review. *J. Mater. Sci. Technol.* **2013**, *29* (6), 489−502.

(25) Gu, X. N.; Li, S. S.; Li, X. M.; Fan, Y. B. Magnesium based degradable biomaterials: A review. *Front Mater. Sci.* **2014**, *8*, 200−218.

(26) Wan, Y.; Xiong, G.; Luo, H.; He, F.; Huang, Y.; Zhou, X. Preparation and characterization of new biomedical magnesium−calcium alloy. *Mater. Des* **2008**, *29*, 2034−2037.

(27) Rad, H. R. B.; Idris, M. H.; Kadir, M. R. A.; Farahany, S. Microstructure analysis and corrosion behaviour of biodegradable Mg−Ca implant alloys. *Mater. Des* **2012**, *33*, 88−97.

(28) Kirkland, N. T.; Birbilis, N.; Walker, J.; Woodfield, T.; Dias, G. J.; Staiger, M. P. In vitro dissolution of magnesium-calcium binary alloys: Clarifying the unique role of calcium additions in bioresorbable magnesium implant alloys. *J. Biomed. Mater. Res. B* **2010**, *95B*, 91−100.

(29) Hassel, T.; Bach, F. W.; Krause, C. Influence of alloy composition on the mechanical and electrochemical properties of binary Mg-Ca alloys and its corrosion behaviour in solutions at different chloride concentrations. In *Proceedings of the 7th International Conference on Magnesium Alloys and Their Applications*; Kainer,

K. U., Ed.; Wiley-VCH Verlag GmbH &Co.: Hoboken, NJ, 2007; pp 789−795.

(30) Kainer, K. U.; Lach, E.Deformation behavior of AZ alloys at high strain rates. In *Magnesium Alloys and Their Applications*; Mordike, B. L., Kainer, K. U., Ed.; Werkstoff-Informationsgesellschaft: Frankfurt, Germany, 1998; pp 369−374.

(31) Drynda, A.; Hassel, T.; Hoehn, R.; Perz, A.; Bach, F. W.; Peuster, M. Development and biocompatibility of a novel corrodible fluoride-coated magnesium-calcium alloy with improved degradation kinetics and adequate mechanical properties for cardiovascular applications. *J. Biomed. Mater. Res., Part A* 2010, 93, 763−775.

(32) Li, Z. J.; Gu, X. N.; Lou, S. Q.; Zheng, Y. F. The development of binary Mg−Ca alloys for use as biodegradable materials within the bone. *Biomaterials* 2008, 29, 1329−1344.

(33) Salahshoor, M.; Guo, Y. Biodegradable orthopaedic magnesium calcium (MgCa) alloys, processing, and corrosion performance. *Materials* 2012, 5, 135−155.

(34) Gu, X. N.; Li, X. L.; Zhou, W. R.; Cheng, Y.; Zheng, Y. F. Microstructure, biocorrosion and cytotoxicity evaluations of rapid solidified Mg−3Ca alloy ribbons as a biodegradable material. *Biomed. Mater.* 2010, 5 (3), 035013.

(35) Yu, H.; Yu, H.-s.; Kim, Y.-m.; You, B.-s.; Min, G.-h. Hot deformation behaviour and processing maps of Mg-Zn-Cu-Zr magnesium alloy. *Trans. Nonferrous Met. Soc. China* 2013, 23 (3), 756−764.

(36) Patil, H. S.; Patel, D. C. Age hardening heat treatment behavior of the as cast Mg−Zn−Al alloys. *Frat. Integrita Strutt.* 2021, 15 (57), 350−358.

(37) Buha, J. Mechanical properties of naturally aged Mg-Zn-Cu-Mn alloy. *Mater. Sci. Eng. A* 2008, 489 (1−2), 127−137.

(38) Golmakaniyoon, S.; Mahmudi, R. Microstructure and creep behaviour of the rare-earth-doped Mg-6Zn-3Cu cast alloy. *Mater. Sci. Eng. A* 2011, 528 (3), 1668−1677.

(39) Zhu, H.-m.; Luo, C.-p.; Liu, J.-w.; Jiao, D.-l. Effects of Cu addition on microstructure and mechanical properties of as-cast magnesium alloy ZK60. *Trans. Nonferrous Met. Soc. China* 2014, 24 (3), 605−610.

(40) Liu, C.; Fu, X.; Pan, H.; Wan, P.; Wang, L.; Tan, L.; Wang, K.; Zhao, Y.; Yang, K.; Chu, P. K. Biodegradable Mg-Cu alloys with enhanced osteogenesis, angiogenesis, and long-lasting antibacterial effects. *Sci. Rep.* 2016, 6, 27374.

(41) Liao, Y.-g.; Han, X.-q.; Zeng, M.-x.; Jin, M. Influence of Cu on microstructure and tensile properties of 7XXX series aluminium alloy. *Mater. Des.* 2015, 66, 581−586.

(42) Buha, J.; Ohkubo, T. Natural ageing in Mg-Zn (-Cu) alloys. *Metallurgical and Materials Transactions A* 2008, 39 (9), 2259−2273.

(43) Chen, T.-J.; Zhang, D.-H.; Wang, W.; Ma, Y.; Hao, Y. Effects of Y content on microstructures and mechanical properties of as-cast Mg-Zn-Nd alloys. *China Foundry* 2015, 12 (5), 339−348.

(44) Balasubramani, N.; Pillai, U.T.S.; Pai, B.C. Optimization of heat treatment parameters in ZA84 magnesium alloy. *J. Alloys Compd.* 2008, 457 (1−2), 118−123.

(45) Unsworth, W. New magnesium alloys for automobile applications. *Light Metal Age* 1987, 45 (7−8), 10−13.

(46) Park, S. H.; Jung, J.-G.; Yoon, J.; You, B. S. You Influence of Sn addition on the microstructure and mechanical properties of extruded Mg-8Al-2Zn alloy. *Mater. Sci. Eng. A* 2015, 626, 128−135.

(47) Bai, Y.; Fang, C.-f.; Hao, H.; Qi, G.-h.; Zhang, X.-g. Effects of yttrium on microstructure and mechanical properties of Mg-Zn-Cu-Zr alloys. *Trans. Nonferrous Met. Soc. China* 2010, 20, 357−360.

(48) Acer, E.; Çadırlı, E.; Erol, H.; Kırındı, T.; Gunduz, M. Effect of heat treatment on the microstructures and mechanical properties of Al-5.5Zn-2.5Mg alloy. *Mater. Sci. Eng., A* 2016, 662, 144−156.

(49) Santhosh, N.; Praveena, B. A.; Jain, R.; AbulHasan, M.; Islam, S.; Khan, M. A.; Razak, A.; Daniyal, M. Analysis of friction and wear of aluminium AA 5083/ WC composites for building applications using advanced machine learning models. *Ain Shams Eng. J.* 2023, 14, 102090.

(50) Shetty, B. P.; Sudheer Reddy, J.; Praveena, B. A.; Madhusudhan, A. Implementation of Python in the Optimization of Process Parameters of Product Laryngoscope Manufactured in the Injection Mold Machine. in *Emerging Research in Computing, Information, Communication and Applications*; Shetty, N. R., Patnaik, L. M., Prasad, N. H., Eds.; Springer, 2022; pp 625−633.

(51) Vijay Kumar, S.; Girish Prasad, M.; Basavaraj, S.; Avinash, L.; Praveen, B. A.; Shiv Prathap, S. Y.; Varadaraj, K. R.; Arpith, Chacko Prediction of Thermal Conductivity for Al6061 Reinforced with Silicon Carbide and Graphite Using Statistical Approach. In *Recent Advances in Mechanical Engineering.*; Narendranth, S., Mukunda, P. G., Saha, U. K.m Eds.; Springer, 2022; pp 201−208.

(52) Isaac, L. P.; Shivakumar, S.; Umesh, V.; Sasidhar Jangam, S.; Santhosh, N.; Shankar, G.; Praveena, B. A. The design and analysis of helical cross - Axis wind turbine. *AIP Conf. Proc.* 2022, 2421, 020004.

(53) Singh Yadav, S. P.; Lakshmikanthan, A.; Ranganath, S.; Gowdru Chandrashekarappa, M. P.; Anand, P. B.; Shankar, V. K.; Avvari, M. Effect of pin geometry and orientation on friction and wear behavior of nickel-coated EN8 steel pin and Al6061 alloy disc pair. *Adv. Mater. Sci. Eng.* 2022, 2022, 3274672.

(54) Santhosh, N.; Praveena, B. A.; Chandrashekar, A.; Mohanavel, V.; Raghavendra, S.; Basheer, D. Wear behaviour of aluminium alloy 5083/SiC/fly ash inoculants based functional composites− optimization studies. *Mater. Res. Express* 2022, 9, 076513.

(55) Nagaraja, S.; Kodandappa, R.; Ansari, K.; Kuruniyan, M. S.; Afzal, A.; Kaladgi, A. R.; Aslfattahi, N.; Saleel, C. A.; Gowda, A. C.; Bindiganavile Anand, P. Influence of Heat Treatment and Reinforcements on Tensile Characteristics of Aluminium AA 5083/Silicon Carbide/Fly Ash Composites. *Materials* 2021, 14 (18), 5261.

(56) Praveena, B A; Shetty, B. P; Arvind, R; Gagan Deep, J G; Kumar, G. S.; Pavan Kalyan, K; Vasu, V. K.; Lokesh, N Design and Fabrication of a Scaled Down Self Load Pneumatic Modern Trailer. *IOP Conf. Ser.: Mater. Sci. Eng.* 2021, 1013, 012004.

(57) Praveena, B. A.; Ahmed, M. D. M.; Kedambadi, V.; Kempaiah, U. N. The design, optimization and analysis of office Chair Base, based on the European standards. *Int. J. Mech. Prod. Eng. Res. Dev.* 2018, 8, 85−92.

(58) Sampatirao, H.; Radhakrishnapillai, S.; Dondapati, S.; Parfenov, E.; Nagumothu, R. Developments in plasma electrolytic oxidation (PEO) coatings for biodegradable magnesium alloys. *Mater. Today: Proc.* 2021, 46 (2), 1407−1415.

(59) Liu, Y.; Zhang, Y.; Wang, Y.-L.; Tian, Y.-Q.; Chen, L.-S. Research progress on surface protective coatings of biomedical degradable magnesium alloys. *J. Alloys Compd.* 2021, 885, 161001.

(60) Bordbar-Khiabani, A.; Yarmand, B.; Mozafari, M. Improving corrosion behavior and in vitro bioactivity of plasma electrolytic oxidized AZ91 magnesium alloy using calcium fluoride containing electrolyte. *Mater. Lett.* 2020, 258, 126779.

(61) Razavi, M.; Fathi, M.; Savabi, O.; Vashaee, D.; Tayebi, L. In vivo assessments of bioabsorbable AZ91 magnesium implants coated with nanostructured fluoridated hydroxyapatite by MAO/EPD technique for biomedical applications. *Mater. Sci. Eng., C* 2015, 48, 21−27.

(62) M, S.; N, R.; K, V.; L, R. K. Fabrication, characterization and in-vitro evaluation of nanostructured zirconia/hydroxyapatite composite film on zirconium. *Surf. Coat. Technol.* 2014, 238, 58−67.

(63) Hamad, T. I.; Fatalla, A. A.; Waheed, A. S.; Azzawi, Z.; Cao, Y.; Song, K. Biomechanical Evaluation of Nano-Zirconia Coatings on Ti-6Al-7Nb Implant Screws in Rabbit Tibias. *Curr. Med. Sci.* 2018, 38, 530−537.

(64) Boccaccini, A. R.; Keim, S.; Ma, R.; Li, Y.; Zhitomirsky, I. Electrophoretic deposition of biomaterials. *Soc. Interface* 2010, 7, S581−S613.

(65) Razavi, M.; Fathi, M.; Savabi, O.; Vashaee, D.; Tayebi, L. Biodegradable magnesium alloy coated by fluoridated hydroxyapatite using MAO/EPD technique. *Surf. Eng.* 2014, 30, 545−551.

(66) Razavi, M.; Fathi, M.; Savabi, O.; Vashaee, D.; Tayebi, L. In vivo study of nanostructured akermanite/PEO coating on biodegrad-

able magnesium alloy for biomedical applications. *J. Biomed, Mater. Res. A* **2015**, *103*, 1798−1808.

(67) Fattah-alhosseini, A.; Molaei, M.; Nouri, M.; Babaei, K. Antibacterial activity of bioceramic coatings on Mg and its alloys created by plasma electrolytic oxidation (PEO): A review. *J. Magnesium Alloys* **2022**, *10* (1), 81−96.

(68) Zhang, D.; Han, Q.; Yu, K.; Lu, X.; Liu, Y.; Lu, Z.; Wang, Q. Antibacterial activities against Porphyromonas gingivalis and biological characteristics of copper-bearing PEO coatings on magnesium. *J. Mater. Sci. Technol.* **2021**, *61*, 33−45.

(69) Chen, Y.; Dou, J.; Pang, Z.; Zheng, Z.; Yu, C.; Chen, C. Ag-containing antibacterial self-healing micro-arc oxidation coatings on Mg−Zn−Sr alloys. *Chen. Surf. Eng.* **2020**, *37*, 926−941.

(70) Chen, J.; Zhang, Y.; Ibrahim, M.; Etim, I. P.; Tan, L.; Yang, K. In vitro degradation and antibacterial property of a copper-containing micro-arc oxidation coating on Mg-2Zn-1Gd-0.5Zr alloy. *Colloids Surf. B Biointerfaces* **2019**, *179*, 77−86.

(71) He, X.; Zhang, X.; Bai, L.; Hang, R.; Huang, X.; Qin, L.; Yao, X.; Tang, B. Antibacterial ability and osteogenic activity of porous Sr/Ag-containing TiO2 coatings. *Biomed. Mater.* **2016**, *11*, 045008.

(72) Zhang, L.; Guo, J.; Huang, X.; Zhang, Y.; Han, Y. The dual function of Cu-doped TiO2 coatings on titanium for application in percutaneous implants. *J. Mater. Chem. B* **2016**, *4*, 3788−3800.

(73) Wu, H.; Zhang, X.; Geng, Z.; Yin, Y.; Hang, R.; Huang, X.; Yao, X.; Tang, B. Preparation, antibacterial effects and corrosion resistant of porous Cu−TiO2 coatings. *Appl. Surf. Sci.* **2014**, *308*, 43−49.

(74) Zhang, X.; Hang, R.; Wu, H.; Huang, X.; Ma, Y.; Lin, N.; Yao, X.; Tian, L.; Tang, B. Synthesis and antibacterial property of Ag-containing TiO2 coatings by combining magnetron sputtering with micro-arc oxidation. *Surf. Coat. Technol.* **2013**, *235*, 748−754.

(75) Teker, D.; Muhaffel, F.; Menekse, M.; Karaguler, N. G.; Baydogan, M.; Cimenoglu, H. Characteristics of multi-layer coating formed on commercially pure titanium for biomedical applications. *Mater. Sci. Eng. C* **2015**, *48*, 579−585.

(76) Molaei, M.; Babaei, K.; Fattah-alhosseini, A. Improving the wear resistance of plasma electrolytic oxidation (PEO) coatings applied on Mg and its alloys under the addition of nano- and micro-sized additives into the electrolytes: A review. *J. Magnesium Alloys* **2021**, *9* (4), 1164−1186.